

Implementation of an all-electron GW Approximation using the Projector Augmented Wave method: II. Application to the optical properties of semiconductors

B. Arnaud and M. Alouani

Institut de Physique et de Chimie des Matériaux de Strasbourg (IPCMS), 23 rue du Loess, 67037 Strasbourg Cedex, France

(August 17, 2018)

Abstract

We used our previously implemented GW approximation (GWA) based on the all-electron full-potential projector augmented wave (PAW) method to study the optical properties of small, medium and large-band-gap semiconductors: Si, GaAs, AlAs, InP, Mg₂Si, C, and LiCl. The aim being to study the size of both local-field (LF) and the quasi-particle (QP) corrections to the calculated dielectric function obtained using the local density approximation (LDA). We found that while the QP corrections tend to align the calculated structures in the optical spectra with their experimental counterparts, the LF effects don't change these peak positions but systematically reduce the intensities of the so called E_1 and E_2 structures in all the optical spectra. The reduction of the intensity of the E_1 peak worsen the agreement with experiment while that of E_2 improves it. We then show that the local-field correction improves considerably the calculated static dielectric constants of all studied semiconductors. Because the static dielectric constant is a ground state property, the remaining discrepancy with experiment should be attributed to the the LDA itself. On the other hand, as expected, the calculation of the static dielectric constant using the GW quasiparticle energies and including the LF effects is underestimated for all the semiconductors. The excitonic effects should then correct for this discrepancy with experiment.

71.20.Ap, 71.15.Mb, 78.20-e, 78.20.Ci

I. INTRODUCTION

In a preceding paper¹ (referred to as I), we have implemented the so called GWA^{2,3} using the all-electron projected augmented wave and applied it successfully to compute the electronic structure of some small, medium, and large-band-gap semiconductors: Si, GaAs, AlAs, InP, Mg₂Si, C, and LiCl. We have then shown that the GWA accounts for most of the discrepancy between the LDA and experiment regarding the energy position of the conduction states. The remaining discrepancy with experiment is believed to be due either to the way the decoupling of the core and valence electrons is performed or to the non-selfconsistent implementation of our all-electron GW method.

It is then clear that the GWA is a useful method for calculating the quasiparticle properties of materials,^{4–28} and many applications using this method are now available. In particular, it has been successfully used to obtain a variety of physical properties, ranging from the band-width narrowing in alkali-metals, and their clusters,^{21,22} to the understanding of the surface reconstruction of semiconductors^{23,24}, or the orientational disorder and the photoemission spectra of solid C₆₀.¹⁶

Nevertheless, one of the most interesting quasiparticle application is the understanding of the many-body effects on the single particle excitation's spectra, such as the optical spectra of semiconductors, and it is still relatively less explored. In this regards, The recent “ab-initio” inclusion of local-field and excitonic effects in the calculation of some semiconductor dielectric functions is a great achievement.^{29–31} There is, however, no systematic study of the trend of the size of these effects with respect to several types of semiconductors. It is therefore important to study the trend of the local-field contribution to the intensities of the structures observed in the optical spectra of various types of semiconductors.

To date all local-field calculations are based on pseudopotential methods. In particular, Louie, Chelikowsky, and Cohen used the empirical pseudo-potential (EPP) method³² to computed the optical properties of Si. Recently Albrecht *et al.* used the ab-initio PP for Si²⁹, and Gavrilenko and Bechstedt for SiC, Si, and C³³. However, these PP calculations do not agree with the EPP³², and do not provide any definite trend for the size of local-field contribution as a function of the semiconductor's type.

In this paper, we use our newly developed all-electron GWA based on the projector-augmented wave (PAW) method³⁴ to compute the local-field effect on various types of semiconductors. The dynamical dielectric function is computed in the random-phase-approximation (RPA) with and without local-field effects using both the LDA and quasiparticle energies calculated within our GWA method. The aim being a systematic study of the local field effects in all these semiconductors in order to understand its contribution to the macroscopic dynamical dielectric function, to the electron loss energy spectrum, and to the static dielectric constant. The latter being a ground state property, and should, in principle, be well described by an LDA calculation including the local-field effects.

Our paper is organized as follows: In the second section we introduce briefly our method of calculation. In the third section we apply it to determine the optical properties of two distinct semiconductor groups: some small and medium band gap semiconductors: Si, GaAs, AlAs, InP, and Mg₂Si, and some large band gap semiconductors or insulators: C and LiCl. We then compare our results with available calculations and experiments. We will also discuss the computed values of the static dielectric constant using the LDA with and without

local-field effects and the corresponding quasiparticle results. This will lead us to discuss the excitonic effect and its contribution to the calculated quasiparticle static dielectric constants.

II. METHOD OF CALCULATION

A. Quasiparticles within the GW approximation

In this paper, we extend the projector-augmented wave method(PAW)³⁴ for solve the Kohn-Sham equations to the determination of the optical properties of semiconductors. To make a quantitative comparison to experimental results we correct the LDA eigenvalues using the quasiparticle energies. As described in our previous paper¹ we can find the excitation energies of the system by solving a quasiparticle equation instead of locating the poles of the Green's function. The quasiparticle energies $E_n(\mathbf{k})$ are determined from the electron selfenergy operator $\Sigma(\mathbf{r}, \mathbf{r}', E_n(\mathbf{k}))$:

$$(T + V_{ext} + V_h)\psi_{\mathbf{k}n}(\mathbf{r}) + \int d^3r' \Sigma(\mathbf{r}, \mathbf{r}', E_n(\mathbf{k}))\psi_{\mathbf{k}n}(\mathbf{r}') = E_n(\mathbf{k})\psi_{\mathbf{k}n}(\mathbf{r}) \quad (1)$$

Here, T is the kinetic energy operator, V_{ext} is the external (ionic) potential, V_h is the Hartree potential due to the average Coulomb repulsion of the electrons. In the GWA, Σ is approximated by a convolution with respect to the frequency variable of the Green's function, G , with the screened interaction W calculated within the RPA.

B. Dielectric function and local field effect

1. Inclusion of local field effects at the RPA level

In a crystal, which possesses lattice translation symmetry, a small electric perturbation $E_0(\mathbf{q} + \mathbf{G}, \omega)$ of wave vector $\mathbf{q} + \mathbf{G}$ and frequency ω produces responses $E(\mathbf{q} + \mathbf{G}', \omega)$ of wave vectors $\mathbf{q} + \mathbf{G}'$. The \mathbf{G} and \mathbf{G}' being reciprocal lattice vectors. Thus, the dielectric matrix describing these responses, is of the form $\epsilon_{\mathbf{G}', \mathbf{G}}(\mathbf{q}, \omega)$ and it can be written as:

$$E(\mathbf{q} + \mathbf{G}', \omega) = \sum_{\mathbf{G}} \epsilon_{\mathbf{G}', \mathbf{G}}^{-1}(\mathbf{q}, \omega) E_0(\mathbf{q} + \mathbf{G}, \omega) \quad (2)$$

An external macroscopic electric field can be viewed as a perturbation of vanishingly small wave vector \mathbf{q} and, therefore, the screening of the external macroscopic field is given by the matrix element $\epsilon_{\mathbf{0}, \mathbf{0}}^{-1}(\mathbf{q}, \omega)$ of the inverse dielectric matrix. In insulating crystals, this results in a formula for the macroscopic dielectric function:

$$\epsilon(\omega) = \lim_{q \rightarrow 0} \frac{1}{[\epsilon_{\mathbf{G}, \mathbf{G}'}^{-1}(q, \omega)]_{\mathbf{0}, \mathbf{0}}} \quad (3)$$

which can be rewritten as:

$$\epsilon(\omega) = \lim_{\mathbf{q} \rightarrow 0} \epsilon_{0,0}(\mathbf{q}, \omega) - \lim_{\mathbf{q} \rightarrow 0} \sum_{\mathbf{G}, \mathbf{G}' \neq 0} \epsilon_{0, \mathbf{G}}(\mathbf{q}, \omega) \epsilon_{\mathbf{G}, \mathbf{G}'}^{-1}(\mathbf{q}, \omega) \epsilon_{\mathbf{G}', 0}(\mathbf{q}, \omega) \quad (4)$$

The first term of this equation is the interband contribution to the macroscopic dielectric function and the second term represents the local field contribution to ϵ . The determination of the macroscopic dielectric constant amounts to the computation of the inverse of $\epsilon_{\mathbf{G},\mathbf{G}'}(\mathbf{q},\omega)$. Adler and Wiser³⁵ have derived, essentially by an extension of the random-phase approximation (RPA), an approximation to $\epsilon_{\mathbf{G},\mathbf{G}'}$ for longitudinal fields,

$$\epsilon_{\mathbf{G},\mathbf{G}'}(\mathbf{q},\omega) = \delta_{\mathbf{G},\mathbf{G}'} - \frac{8\pi}{\Omega|\mathbf{q} + \mathbf{G}||\mathbf{q} + \mathbf{G}'|} \sum_{\mathbf{k},n,m} \frac{[f_{n,\mathbf{k}-\mathbf{q}} - f_{m,\mathbf{k}}] M_{\mathbf{G}}^{nm}(\mathbf{k},\mathbf{q}) [M_{\mathbf{G}'}^{nm}(\mathbf{k},\mathbf{q})]^*}{E_n(\mathbf{k}-\mathbf{q}) - E_m(\mathbf{k}) + \omega + i\delta} \quad (5)$$

where n and m are the band indices, $f_{n,\mathbf{k}}$ is the zero temperature Fermi distribution, Ω is the crystal volume and $M_{\mathbf{G}}^{nm}(\mathbf{k},\mathbf{q})$ are the matrix elements

$$M_{\mathbf{G}}^{nm}(\mathbf{k},\mathbf{q}) = \langle \Psi_{\mathbf{k}-\mathbf{q}n} | e^{-i(\mathbf{q}+\mathbf{G}) \cdot \mathbf{r}} | \Psi_{\mathbf{k}m} \rangle \quad (6)$$

which are calculated as described in our preceding paper I in the context of the GW approximation. In this expression, the time dependence of the field was assumed to be $e^{-i\omega t}$ and the small positively defined constant δ guarantees that the matrix elements of $\epsilon(\omega)$ are analytic functions in the half upper plane. Such a matrix could be separated into an hermitian part $\epsilon_{\mathbf{G},\mathbf{G}'}^{(1)}$ and an anti-hermitian part $i\epsilon_{\mathbf{G},\mathbf{G}'}^{(2)}$ according to

$$\epsilon_{\mathbf{G},\mathbf{G}'}(\mathbf{q},\omega) = \epsilon_{\mathbf{G},\mathbf{G}'}^{(1)}(\mathbf{q},\omega) + i\epsilon_{\mathbf{G},\mathbf{G}'}^{(2)}(\mathbf{q},\omega) \quad (7)$$

with $\epsilon^{(2)}$ for positive ω given by

$$\epsilon_{\mathbf{G},\mathbf{G}'}^{(2)}(\mathbf{q},\omega) = \sum_{\mathbf{k},v,c} \frac{8\pi^2}{\Omega|\mathbf{q} + \mathbf{G}||\mathbf{q} + \mathbf{G}'|} M_{\mathbf{G}}^{vc}(\mathbf{k},\mathbf{q}) [M_{\mathbf{G}'}^{vc}(\mathbf{k},\mathbf{q})]^* \delta(\omega - [E_c(\mathbf{k}) - E_v(\mathbf{k}-\mathbf{q})]) \quad (8)$$

and $\epsilon^{(1)}$ defined by a Kramers Kronig (KK) transform as

$$\epsilon_{\mathbf{G},\mathbf{G}'}^{(1)}(\mathbf{q},\omega) = \delta_{\mathbf{G},\mathbf{G}'} + \frac{2}{\pi} P \int_0^\infty d\omega' \frac{\omega' \epsilon_{\mathbf{G},\mathbf{G}'}^{(2)}(\mathbf{q},\omega')}{\omega'^2 - \omega^2} \quad (9)$$

It should be noted here that the matrix elements of $\epsilon^{(2)}$ and $\epsilon^{(1)}$ could be chosen to be real if the inversion is contained in the point group of the crystal. The calculation of the head element $\lim_{\mathbf{q} \rightarrow 0} \epsilon_{\mathbf{0},\mathbf{0}}^{(2)}(\mathbf{q},\omega)$ and of the wing elements $\lim_{\mathbf{q} \rightarrow 0} \epsilon_{\mathbf{0},\mathbf{G}}^{(2)}(\mathbf{q},\omega)$ necessitate special care if we want to determine the optical properties of semiconductors when the GW approximation or the scissors-shift approximation is used to determine the electronic structure. Instead of handling numerically $\lim_{\mathbf{q} \rightarrow 0} M_{\mathbf{0}}^{nm}(\mathbf{k},\mathbf{q})/q$ where the quasiparticle wave functions $\psi_{\mathbf{k}n}$ and the quasiparticle energies $E_n(\mathbf{k})$ are to be used, it is reasonable to approximate the quasiparticle wave function with the LDA wave function, and take the limit analytically³⁶:

$$\lim_{\mathbf{q} \rightarrow 0} M_{\mathbf{0}}^{nm}(\mathbf{k},\mathbf{q})/q = \hat{\mathbf{q}} \cdot \langle n\mathbf{k} | \mathbf{p} | m\mathbf{k} \rangle / (\epsilon_m(\mathbf{k}) - \epsilon_n(\mathbf{k})) \quad (10)$$

Here $|n\mathbf{k}\rangle$ and $\epsilon_n(\mathbf{k})$ are the LDA wave functions and energies for band n and wave vector \mathbf{k} , respectively. Indeed, it was shown by inspection that for Si the LDA and the GW wave functions have more than 99% overlap⁴. If the scissors-shift approximation is used, it is easy to show that

$$\epsilon_{\mathbf{G},\mathbf{G}'}^{(2)GW}(\omega) = \epsilon_{\mathbf{G},\mathbf{G}'}^{(2)LDA}(\omega - \Delta) \quad (11)$$

where Δ defines the rigid shift of the conduction bands with respect to the valence bands.

In the above formalism we have neglected the exchange-correlation contribution to the dielectric function. The calculation of this contribution amounts basically to the determination of the exchange-correlation kernel $K_{xc}(\mathbf{r}, \mathbf{r}') = \partial^2 E_{xc} / \partial \rho(\mathbf{r}) \partial \rho(\mathbf{r}') = dV_{xc} / d\rho|_{\rho(\mathbf{r})} \delta(\mathbf{r} - \mathbf{r}')$, where E_{xc} and V_{xc} are the exchange-correlation energy and potential, respectively, and $\rho(\mathbf{r})$ is the charge density at \mathbf{r} . The calculation of K_{xc} is much more complicated in all-electron than in a pseudo-potential method, since one has to determine the matrix of the Kernel in the Fourier space. Indeed, the FFT of the exchange-correlation kernel converges very slowly with the number of \mathbf{G} -vectors in reciprocal space because of the oscillating nature of the charge density in real space. Fortunately, it has been shown that this kernel contribution to the total dielectric function is small.^{5,33}

2. numerical details

The size of the dielectric matrix is critical for the convergence of the optical spectrum. We have found that a size of 65×65 for all systems studied here is good for the convergence of the optical spectra, except for LiCl where the convergence was achieved for a matrix size of 181×181 . The imaginary part of each matrix element $\epsilon_{\mathbf{G},\mathbf{G}'}^{(2)}(\mathbf{q} \rightarrow 0, \omega)$ is evaluated in energy intervals of 0.1 eV up to 200 eV. Then the 'real part' $\epsilon^{(1)}$ is deduced via a KK transformation defined previously (see Eq. (9)). The linear tetrahedron method^{37,38} is employed to perform the summation over the Brillouin zone which appears in Eq. (8). We use 8000 \mathbf{k} -points in the full Brillouin zone to calculate the head element and 1000 \mathbf{k} -points to calculate the wing elements and the body elements. The hermiticity of $\epsilon_{\mathbf{G},\mathbf{G}'}^{(2)}(\mathbf{q} \rightarrow 0, \omega)$, the time reversal symmetry and the symmetry properties are used to reduce the number of matrix elements to be computed.

III. RESULTS AND DISCUSSION

A. Calculated optical spectra with and without local-field effects

The dynamical dielectric function of all the semiconductors studied here are calculated using Eq. (4). The local-field effects are represented by the second term on the right of this equation. To test the accuracy of the all-electron PAW method we have computed the imaginary-part of the dielectric function of Si and GaAs without local field and compared them to the full-potential linear muffin-tin (FPLMTO) results⁴⁰. Fig. 1 shows that the agreement with the FPLMTO spectra is excellent. These results are interesting because they set, for the first time, the standard for an accurate LDA dielectric function of Si and GaAs computed by two different all-electron methods. This is encouraging since the LMTO method is a state-of-the-art first principles method for electronic structure, and in comparison, the PAW formalism is much simpler, but nevertheless the method doesn't loss any accuracy.

Before presenting our calculated optical properties of semiconductors, we would like to mention the different ways we have obtained the optical spectra: (1) We have used our

LDA calculated band structure to directly compute the optical spectra. (2) We have used the so called scissors-operator energy shift to the LDA eigenvalues. The value of the shift corresponds to our GWA correction of the LDA direct band gap at the Γ point. (3) Finally, we used the GWA calculated quasiparticle energies across the Brillouin zone. All these three types of calculations were produced with and without local-field effects.

The accuracy of the macroscopic function depends on the convergence of all the elements of the microscopic dielectric matrix. As stated in the previous section we have found that a matrix of 65 by 65 \mathbf{G} -vectors and the use of 200 bands in the interband transitions produce a well converged $\epsilon(\omega)$, except for LiCl where a matrix of 181×181 \mathbf{G} -vectors is used. Fig. 2 shows different elements of the microscopic dielectric function of Silicon versus photon energy up to 70 eV. The highest intensity of these elements is at least one order of magnitude smaller than the $\epsilon_{(000),(000)}$ element. We compared our results to these of Gavrilenko and Bechstedt³³ and found that the agreement with their results is only at the semi-quantitative level. We are surprised to find that Gavrilenko and Bechstedt have a relatively large intensity in the band gap of their $Im\epsilon_{(000),(111)}$ and $Im\epsilon_{(111),(200)}$.

Fig. 3 shows the calculated real and imaginary part of the dielectric function of Si versus photon energy up to 10 eV with and without LF and QP energy shift. These calculations are compared to the experimental results of Aspnes and Studna.⁴⁴ The dashed curve represent the difference between the calculated optical spectra using the calculated GW quasiparticle energies and the one obtained using the scissors-operator energy shift to the LDA eigenvalues. This spectral difference is small justifying the use of the scissors-operator for the calculation of the optical spectra of small and medium gap semiconductors. Because of this small change of the dielectric function due to the use of the quasiparticle energies, and because of the high CPU cost in obtaining the quasiparticle energies across the whole Brillouin zone, all the other small and medium gap semiconductors are calculated using only the scissors-operator shift. Notice that the agreement concerning the peak positions is fortuitous, because the QP energy shift underestimates the direct band gap at Γ (for details, see paper I). A calculation with an energy shift which reproduces the experimental band gap will slightly overestimates the peak positions by about 0.3 eV, and this overestimation is valid for all semiconductors studied here. It is also worth mentionning that our preliminary calculation of the excitonic effects shows that in the case of Si the E_1 , and E_2 peaks are shifted by about 0.2 eV towards lower photon energies, and the agreement with experiment concerning the postions and intensities of these peaks is recovered.

On the other hand, in agreement with the empirical pseudopotential (EPP) calculation of Louie, Chelikowsky and Cohen we have found that the LF effects do not change the position of the structures present on the optical spectrum³². But the intensities of the so called E_1 and E_2 peaks are reduced, again in agreement with the EPP. Thus the local-field effects seem to improve the agreement with experiment regarding the intensity of the E_2 peak and the structures in the higher energy part, and worsen the agreement with experiment regarding the low energy part where the E_1 peak is located. It is surprising that our calculations do not agree well with the ab-initio PP calculation of Gavrilenko and Bechstedt³³ which is supposed to be similar to the EPM calculation. The latter calculation found that while the LF underestimates the E_1 peak intensity in agreement with our calculation and EPP, it overestimates the E_2 peak intensity in disagreement with our calculation and with EPP. The calculated spectrum of Albrecht *et al.*²⁹, obtained by solving the Bethe-Salpeter equation,

using the PP method, in a special limit where only local-field effects are included, agrees only qualitatively with our calculation and the EPP results³². Their E'_1 structure, which is located in energy above the E_2 structure, has a large intensity and disagrees with our calculation and other ab-initio or EPP calculations^{40,32}. It is then not clear what makes the extra reduction of their E'_1 peak when the excitonic effects are included.

We have performed similar calculations for GaAs, AlAs, InP, Mg₂Si, C and LiCl, which we present in Figs. 4, 5, 6, 7, 8, and 9 and compare to available experimental results^{44,45}. For all these semiconductor the scissors-operator energy shift, corresponding to the difference between the quasiparticle and LDA eigenvalues at the Γ point, is used to produce the quasiparticle optical spectra, except for C where we have represented the dielectric function obtained using the GW quasiparticle energies at each point in the Brillouin zone. In this latter case the difference between the optical spectra, calculated using the GW quasiparticle energies and the scissors-operator energy shift, is shown by a dashed curve in Fig. 8, and it is found to be much larger than in the case of Si. We believe that the same conclusion should be valid for LiCl, however due to the cost of the GW calculation and the absence of the experimental results we preferred not to perform the calculation with the quasiparticle energies. Moreover, the small dielectric constants of these two large gap semiconductors indicate that excitonic effects are important. For example, the large discrepancy between our calculated spectra of Diamond and experiment can be attributed to these effects.

In conclusion, the most important trend of the LF on the optical spectra of all types of semiconductors studied here, is that: The E_1 's intensity reduction disagrees with experiment, whereas the E_2 's intensity reduction agrees well with experiment whenever available. It is interesting to notice that for the insulator LiCl the LF effects seem to reduce substantially the intensities of the peaks at the low photon energy.

B. Electron-energy-loss function

Figs. 11, 12 show our calculated electron-energy-loss (EEL) functions $-Im[\epsilon^{-1}(q = 0, \omega)]_{0,0}$ for small-band-gap semiconductors: Si, GaAs, AlAs, InP, and Mg₂Si and large-band-gap semiconductors: C and LiCl, respectively. The calculation are done within the LDA with and without the local-field effect. Whenever possible the calculation is compared to available energy-loss spectra. The local-field effects seems to improve the agreement with experiment by reducing significantly the intensity of the main peak. The EEL functions of C and specially of LiCl are much complicated. The LDA C EEL function has two maxima at 31.5 and 34.5 eV and these values are shifted to 31.4 and 35.2 eV, respectively, when the LF effects are included. The experimental curve seems to present only one resonance at 32 eV. This discrepancy, could be easily due to small unaccuracy in the calculated dielectric function at these high photon energies.

We did not calculate $-Im[\epsilon^{-1}(q = 0, \omega)]_{0,0}$ for the quasi-particle energy because we believe that GWA is not valid at high energies and as pointed out in Ref.⁴⁰ the plasma resonance will be pushed towards higher energies in disagreement with experiment. This because the electronic structure at higher energy is most probably much better described using the LDA than the GWA because: (1) at these higher energies the scattering of an electron with the atomic potential is small. In this respect, these high electronic states can

be obtained from an almost free-electron theory. (2) the plasmon-pole model is not valid at these high energies.

Table I shows the values of the maxima of the energy-loss function compared to the experimental results obtained from the EEL experiments^{41,42} and from the measured dielectric function⁴³. The free-electron plasma frequency is also shown for comparison. The plasma resonance of the EEL spectra of Si and GaAs are in good agreement with experiment and with the free-electron plasma frequency. The energy electron-energy-loss function of LiCl is too complicated containing many peaks, and in the absence of experimental data we prefered not to show the values of these maxima in table I.

C. The static dielectric constant

The static dielectric function ϵ_∞ with or without local-field effects is computed using the Kramers-Kroenig relations. The calculations were produced using the RPA dielectric function and performing analytically the limit $\mathbf{q} \rightarrow 0$. Table II presents ϵ_∞ for all semiconductors studied here and compares them to other calculations^{5,39,40,46–48} and to available experimental results⁴⁹. To illustrate our data and stress the agreement with experiment we show in Fig. 10 all our calculated results versus experiment, except for Mg₂Si were we are not aware of any available experimental result. A perfect agreement with experiment is achieved when the calculated value is on the dashed line. Because the static dielectric function is a ground state property, we expect that the calculation with LDA including the LF effect should reproduce the experimental results. However, we observe only an improvement due to this effect. We conclude that the remaining of the discrepancy with experiment is due to the used of the LDA itself instead of the full density functional theory. Notice that for large band gap semiconductors, the LDA results including the LF effects are in good agreement with experiment. This trend was also observed by other researchers^{40,50}.

On the other hand, the quasiparticle description of the static dielectric constant, is of importance, since it will be directly compared to LDA results. A comparison to experiment will show whether the excitonic effect corrections are important or not. In this respect we notice that, when the GWA energy shift and LF effects are both included, the QP calculation slightly underestimates the static dielectric function for all the semiconductors studied here regardless of the size of the band gap or the type of semiconductor. This suggests, effectively, the importance of the excitonic effects which are expected to produce a positive contribution leading to a better agreement with experiment. This positive contribution arises from the reduction of the optical band gap from its GWA counterpart, and to the transfer of the force of the oscillator towards lower photon energies. It is however interesting to remark that since for large band gap materials (C and LiCl) the static dielectric function within LDA including LF effects agrees nicely with experiment, the excitonic contribution should cancel out the QP correction.

IV. CONCLUSION

We have used our previously implemented GWA within the all-electron projected augmented wave method (PAW) to study the optical properties of some small, medium and

large-band-gap semiconductors: GaAs, AlAs, InP, Mg₂Si, C and LiCl. In general, the inclusion of the the quasiparticle (QP) energy shift and the local-field (LF) effects improves the agreement with experiment. In particular, the LF effects reduce the intensities of the so called E_1 and E_2 peaks without changing their energy positions. This reduction of the peak intensity worsen the agreement for the E_1 peak but improves it for the E_2 peak. This trend is observed for all the studied semiconductors and is found to be in agreement with the empirical pseudopotential (EPP) calculation of Louie, Chelikowsky and Cohen³². The QP energy shift pushes the calculated peaks towards higher energies in agreement with experiment. However, because the calculated GWA energy shift does not always produce the correct experimental band gaps, the agreement of the peak positions with experiment in the case of Si, GaAs, and Mg₂Si is fortuitous. A calculation using an energy shift which reproduces the experimental band gap will produce theoretical peaks slightly higher in energy compared to experiment. On the other hand, our preliminary calculation of the excitonic effects for Si shows that the E_1 , and E_2 peaks are shifted by about 0.2 eV towards lower photon energies, and the agreement with experiment concerning the postions and intensities of these peaks is is recovered. Thus, the slight shift of the peaks at higher energy, when the experimental band gaps are used, is canceled by the excitonic effects.

The static dielectric function ϵ_∞ with or without local-field effects is computed using the Kramers-Kroenig relations. The calculation were performed using the RPA dielectric function and performing analytically the limit $\mathbf{q} \rightarrow 0$. Because the static dielectric function is a ground state property, the calculation using LDA and including the LF effect should reproduce the experimental results. In our calculations, for small and medium band gap semiconductors, we observe only an improvement due to this effect, and concluded that the remaining of the discrepancy is due to the use of the LDA itself instead of the full density functional theory. However, for large band gap semiconductors, the LDA results including the LF effects are in good agreement with experiment.

On the other hand, the QP calculation, when both the GWA energy shift and LF effects are included, underestimated the static dielectric function for all the semiconductors studied here. This suggests the importance of the excitonic effects which are expected to produce a positive contribution.

V. ACKNOWLEDGMENT

We would like to thank P. Blöchl for providing us with his PAW code and for useful discussions. Part of this work was done during our visit to the Ohio State University, and we would like to thank J. W. Wilkins and W. Aulbur for useful discussions. The Supercomputer time was granted by CINES on the IBM SP2 supercomputer (project gem1100).

REFERENCES

- ¹ B. Arnaud and M. Alouani, preceding paper, submitted to Phys. Rev. B
- ² L. Hedin, Phys. Rev. **139**, A796 (1965).
- ³ L. Hedin and S. Lundquist, in *Solid State Physics*, edited by H. Ehrenreich, F. Seitz, and D. Turnbull (Academic, New York, 1969), Vol. 23, p. 1.
- ⁴ M. S. Hybertsen and S. G. Louie, Phys. Rev. B **34**, 5390 (1986); Comments Cond. Mat. Phys. **13**, 223 (1987).
- ⁵ M. S. Hybertsen and S. G. Louie, Phys. Rev. B **35**, 5585 (1987).
- ⁶ R. W. Godby, M. Schlüter, and L.J. Sham, Phys. Rev. B **37**, 10159 (1988).
- ⁷ R. W. Godby, and M. Schlüter, Phys. Rev. B **35**, 4170 (1987).
- ⁸ R. W. Godby, and R.J. Needs, Phys. Rev. Lett. **62**, 1169 (1989).
- ⁹ W. von der Linden, P. Fulde, and K.-P. Bohnen, Phys. Rev. B **34**, 1063 (1986).
- ¹⁰ W. von der Linden and P. Horsch, Phys. Rev. B **37**, 8351, 8351 (1988).
- ¹¹ R. T. Ummels, P. A. Bobbert and W. van Haeringen, Phys. Rev. B **57**, 11962 (1998).
- ¹² P. A. Bobbert and W. van Haeringen, Phys. Rev. B **49**, 10326 (1994).
- ¹³ N. Hamada, M. Hwang and A.J. Freeman, Phys. Rev. B **41**, 3620 (1990).
- ¹⁴ R. Hott, Phys. Rev. B **44**, 1057 (1991).
- ¹⁵ F. Aryasetiawan, Phys. Rev. B **46**, 13051 (1992).
- ¹⁶ E. L. Shirley and S. G. Louie, Phys. Rev. Lett. **71**, 331993.
- ¹⁷ E. L. Shirley, X. Zhu, and S. G. Louie, Phys. Rev. Lett. **69**, 2955 (1992).
- ¹⁸ F. Aryasetianwan and O. Gunnarsson, Rep. Prog. Phys. **61**, 237-312 (1998).
- ¹⁹ W. G. Aulbur, L. Jönsson, and J. W. Wilkins, 'Quasiparticle calculations in solids', to be published in Solid state Physics; edited by H. Ehrenreich.
- ²⁰ W. G. Aulbur, PhD thesis, The Ohio State University, 1996.
- ²¹ J. E. Northrup, M. S. Hybertsen, and S. G. Louie, Phys. Rev. B **39**, 8198 (1989).
- ²² S. Saito, S. B. Zhang, S. G. Louie, and M. L. Cohen, Phys. Rev. B **40**, 3643 (1989).
- ²³ X. Zhu and S. G. Louie, Phys. Rev. B **43**, 12146 (1991).
- ²⁴ J. E. Northrup, Phys. Rev. B **47**, 10032 (1993).
- ²⁵ S. B. Zhang, M. L. Cohen, S. G. Louie, D. Tománek, and M. S. Hybertsen, Phys. Rev. B **41**, 10058 (1990).
- ²⁶ S. B. Zhang, M. S. Hybertsen, M. L. Cohen, S. G. Louie, and D. Tománek, Phys. Rev. Lett. **63**, 1495 (1989).
- ²⁷ E. L. Shirley and R. M. Martin, Phys. Rev. B **47**, 15404 (1993).
- ²⁸ J. P. A. Charlesworth, R. W. Godby, R. J. Needs, L. J. Sham, Mat.Science and Eng. B-Solid State Mat. Adv. Tech. **14**, 262 (1992).
- ²⁹ S. Albrecht, L. Reining, R. Del Sole, and G. Onida, Phys. Rev. Lett. **80**, 4510 (1998).
- ³⁰ L. X. Benedict, E. L. Shirley, and R. B. Bohn, Phys. Rev. Lett. **80**, 4514 (1998); Phys. Rev. B **57**, R9385 (1998).
- ³¹ M. Röhlfing and S. G. Louie, Phys. Rev. Lett. **81**, 2312 (1998).
- ³² S. Louie, J. R. Chelikowsky, and M. L. Cohen, Phys. Rev. Lett. **34**, 155 (1975).
- ³³ V. I. Gavrilenko and F. Bechstedt, Phys. Rev. B **55**, 4343 (1997); *ibid*, **54**, 13416 (1996). Notice that legend of Fig. 4 and hence these of Figs. 5 and 6 of their 1997 PRB paper is wrong. The legend should read: "Dashed line: with LF and XC effects; solid line: without LF and XC effects (only $\mathbf{G} = \mathbf{G}' = 0$).
- ³⁴ P.E Blöchl, Phys. Rev. B **50**, 17953 (1994).

³⁵ S.L. Adler, Phys. Rev. **126**, 413 (1962); N. Wiser, Phys. Rev. **129**, 62 (1963).

³⁶ R. Del Sole and R. Girlanda, Phys. Rev. B **48**, 11789 (1993).

³⁷ O. Jepsen and O. K. Andersen, Solid State Commun. **9**, 1763 (1971); G. Lehmann and M. Taut, Phys. Status Solidi B **54**, 469 (1972).

³⁸ A. H. MacDonald, S. H. Vosko and P.T Coleridge, J. Phys. C **12**, 2991 (1979).

³⁹ M. Rohlfing, Peter Krüger and J. Pollmann, Phys. Rev. B **48**, 17791 (1993).

⁴⁰ M. Alouani and J. M. Wills, “*Excited states calculated by means of the linear muffin-tin orbital method*”, Springer series (to be published); Phys. Rev. B. **54**, 2480 (1996).

⁴¹ H. Raether, *Excitation of Plasmons and interband Transitions by Electrons*, Springer Tracts in Modern Physics vol. 88 (Springer, New York, 1980).

⁴² H. R. Phillips and A. Taft, Phys. Rev. **136**, A1445 (1964).

⁴³ H. R. Philipp and H. Ehrenreich, Phys. Rev. **129**, 1550 (1963).

⁴⁴ D.E. Aspnes and A. A. Studna, Phys. Rev. B **27**, 985 (1983).

⁴⁵ A. D. Papadopoulos and E. Anastassakis, Phys. Rev. B **43**, 5090 (1991).

⁴⁶ Z. H. Levine, and D. C. Allan, Phys. Rev. Lett. **63**, 1719 (1989).

⁴⁷ J. E. Raynolds, Z. H. Levine, and J. W. Wilkins, Phys. Rev. B **51**, 10477 (1995).

⁴⁸ Z. H. Levine, and D. C. Allan, Phys. Rev. Lett. **66**, 41 (1991).

⁴⁹ *Numerical Data and Functional Relationships in Science and Technology*, edited by K.H. Hellwege and O. Madelung, Landolt-Börnstein, New Series, Group **III**, Vols. 17a and 22a (Springer, Berlin, 1982).

⁵⁰ J. Chen, Z. H. Levine, and J. W. Wilkins, Appl. Phys. Lett. **66**, 1129 (1995).

TABLES

TABLE I. Influence of LF on the energy position of the plasmon peak of the electron-energy-loss spectra. Our calculation is compared to available experimental results and to the free-electron plasma frequency (in eV).

Material	LDA	LDA+LF	Free electron	Expt.
Si	16.6	16.5	16.6	16.4 ^a , 16.9 ^b
GaAs	16.8	16.4	15.6	14.7 ^a
AlAs	16.45	15.8	15.8	
InP	15.5	15.0	14.8	
Mg ₂ Si	12.65	12.5	13.0	
C	31.5 and 34.5	31.4 and 35.2	31.2	32 ^c

^aRef.⁴³, ^bRef.⁴¹, ^cRef.⁴²

TABLE II. Influence of LF and QP shifts on the macroscopic dielectric constant ϵ_∞ compared to other calculations and to experiment.⁴⁹

Material	LDA	LDA+LF	QP shift	QP shift+LF	Expt.		
Si	13.78	13.6 ^a , 13.8 ^b	12.39	12.2 ^a , 12.4 ^b	12.04	10.92	11.7
Si		13.75 ^f , 12.8 ^c					
GaAs	14.23	13.1 ^c , 14.17 ^d	12.78		11.61	10.51	10.9
AlAs	10.20	9.5 ^e	8.93	8.65 ^e	8.55	7.59	8.2
InP	10.71		9.55		8.91	8.01	9.6
Mg ₂ Si	17.73		15.22		15.79	13.56	
C	5.94	5.5 ^c	5.54	5.62 ^a	5.25	4.94	5.7
LiCl	3.35		2.84	2.9 ^a	2.82	2.46	2.7

^aRef.⁵, ^bRef.⁴⁶, ^cRef.³⁹ ^dRef.⁴⁷, ^eRef.⁴⁸, ^fRef.⁴⁰.

FIGURES

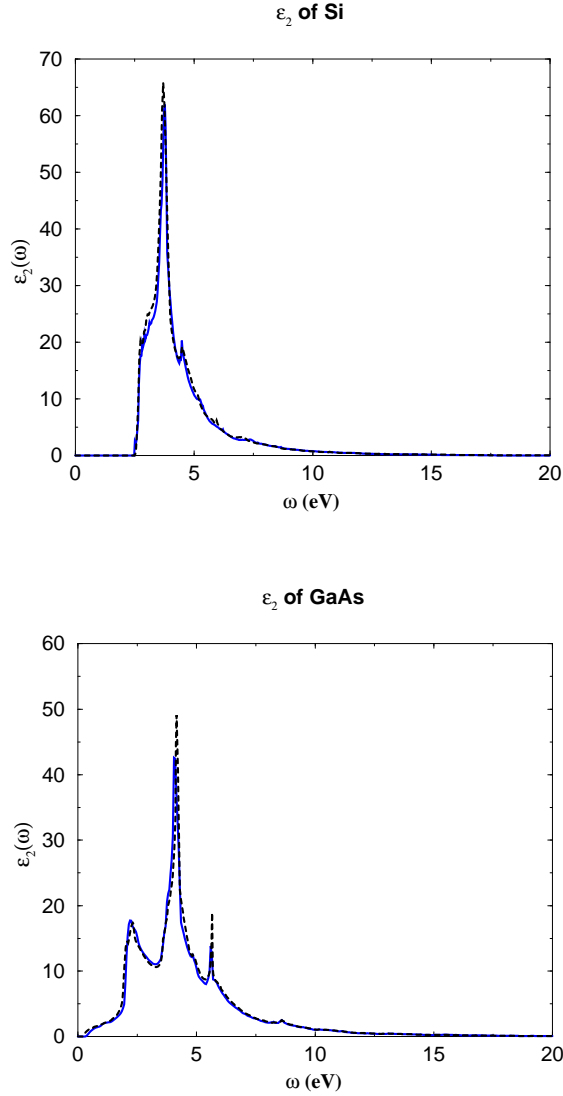


FIG. 1. Calculated LDA imaginary part of the Dielectric function of Si and GaAs versus photon energy using PAW method (solid line) and the FPLMTO method⁴⁰ (dashed line). The agreement between the two calculations is excellent. This sets for the first time the LDA results of the dielectric functions of Si and GaAs.

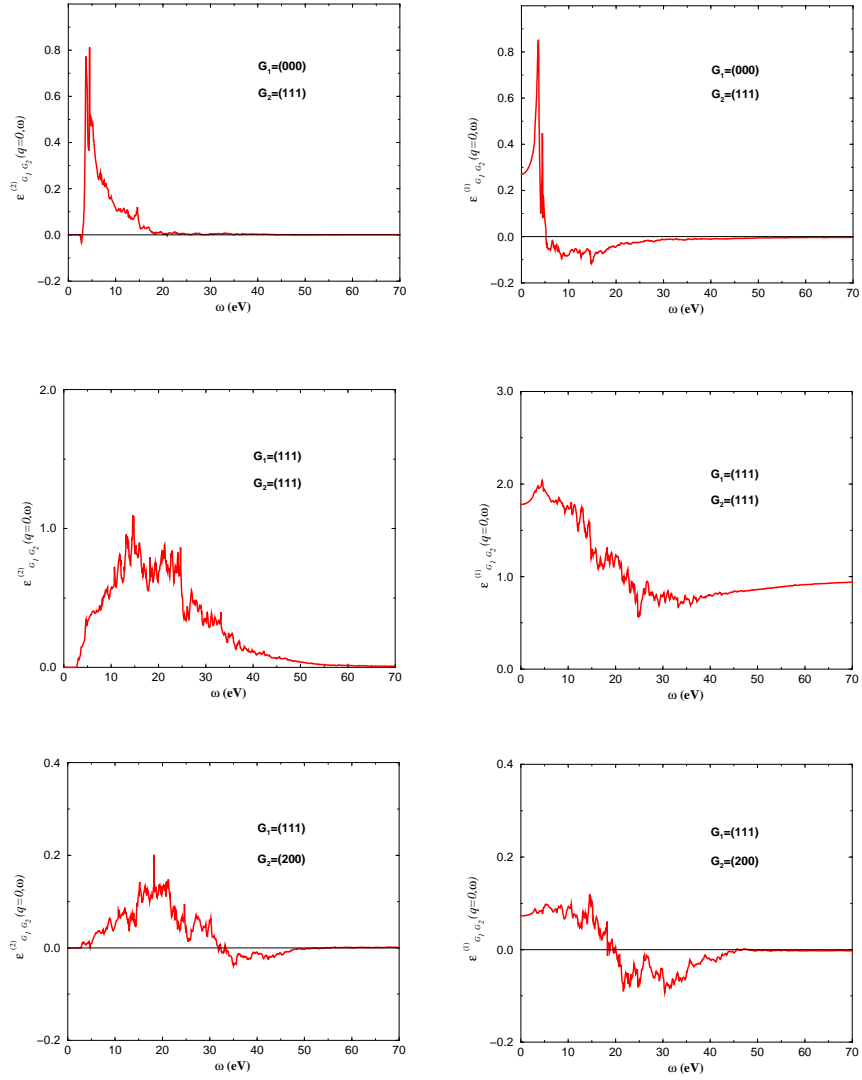


FIG. 2. Calculated elements of the real (right column) and imaginary part (left column) of the symmetrized microscopic dielectric matrix $\epsilon(\mathbf{q}, \omega)_{\mathbf{G}, \mathbf{G}'}$ of Silicon for the limit $\mathbf{q} \rightarrow \mathbf{0}$ and for $(\mathbf{G}, \mathbf{G}') = (000, 111)$, $(111, 111)$, and $(111, 200)$.

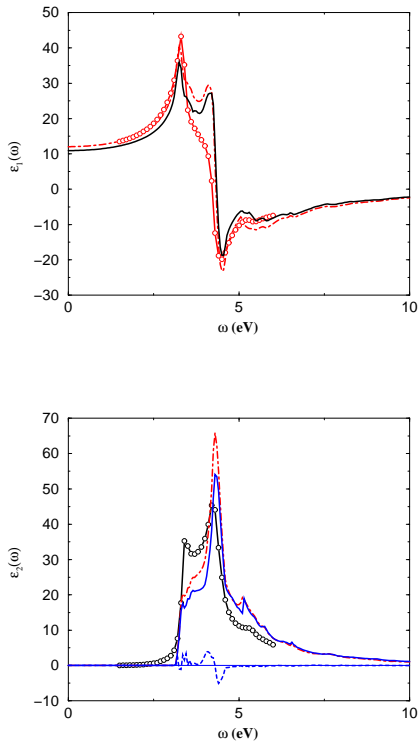


FIG. 3. Calculated real and imaginary part of the dielectric function of Si versus photon energy. The dot-dashed line is our calculation using a rigid energy shift of 0.6 eV of the LDA conduction bands, corresponding to our calculated GW band gap correction at the Γ point. The solid line is the calculation with a rigid energy shift of the conduction bands and including the local-field effects. The solid line with open circles is the experimental data⁴⁴. The dashed curve is the difference between the calculation using the quasiparticle energy across the Brillouin zone and that using the rigid energy shift. This small difference justifies the use of the scissors-energy shift for the calculation of the optical properties.

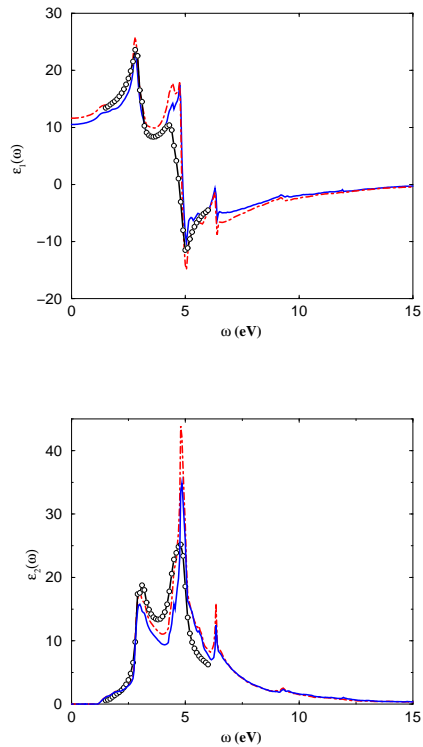


FIG. 4. Calculated real and imaginary part of the Dielectric function of GaAs versus photon energy. The dot-dashed line is our calculation using a rigid energy shift of 0.75 eV of the LDA conduction bands, corresponding to our calculated GW band-gap correction at the Γ point. The solid line is our calculation using the rigid energy shift and including the local-field effects. The solid line with open circles is the experimental spectrum⁴⁴.

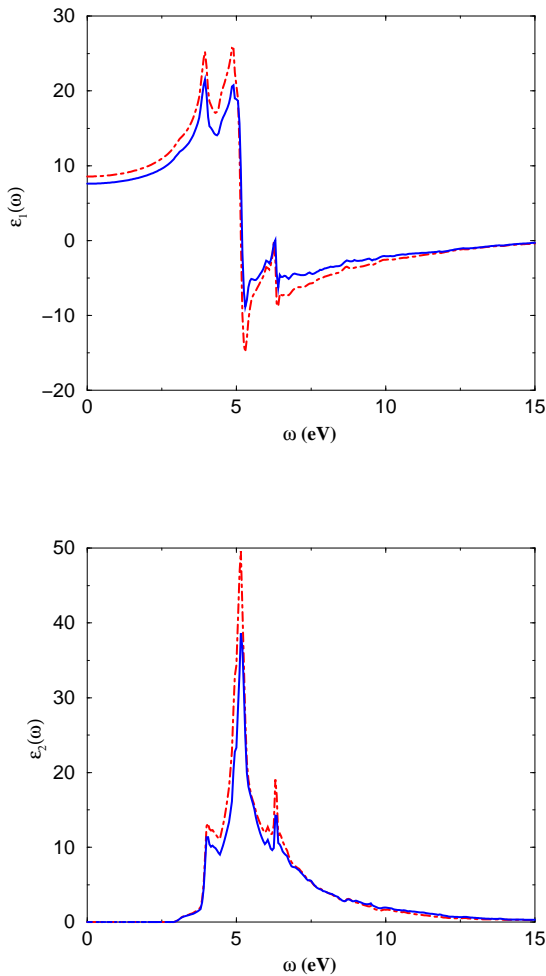


FIG. 5. Calculated real and imaginary part of the dielectric function of AlAs versus photon energy. The dot-dashed line is our calculation using a rigid energy shift of 0.95 eV of the LDA conduction bands, corresponding to our calculated GW band gap correction at the Γ point. The solid line is our calculation with a rigid energy shift and including the local-field effects.

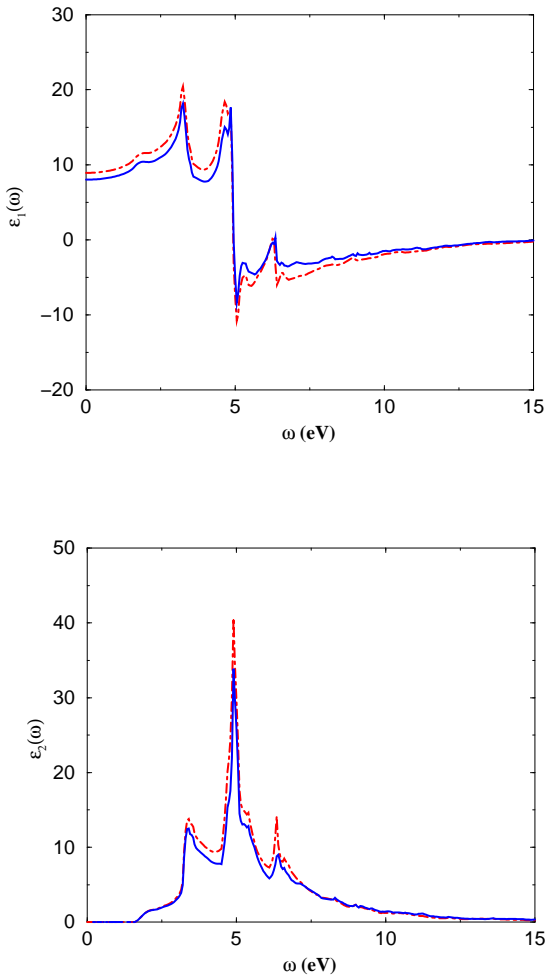


FIG. 6. Calculated real and imaginary part of the dielectric function of InP versus photon energy. The dot-dashed line is our calculation using a rigid energy shift of 0.8 eV of the LDA conduction bands, corresponding to our calculated GW band gap correction at the Γ point. The solid line is our calculation with a rigid energy shift and including the local-field effects.

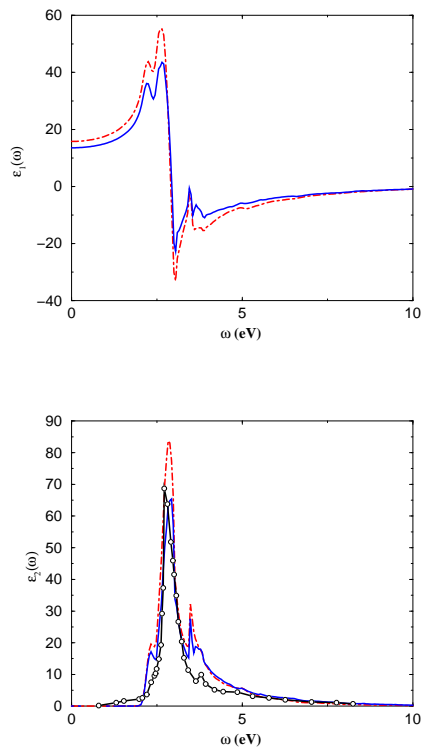


FIG. 7. Calculated real and imaginary part of the dielectric function of Mg_2Si versus photon energy. The dot-dashed line is our calculation using a rigid energy shift of 0.33 eV of the LDA conduction bands, corresponding to our calculated GW band gap correction at the Γ point. The solid line is our calculation with a rigid energy shift and including the local-field effects. The solid line with open circles is the experimental spectrum⁴⁴.

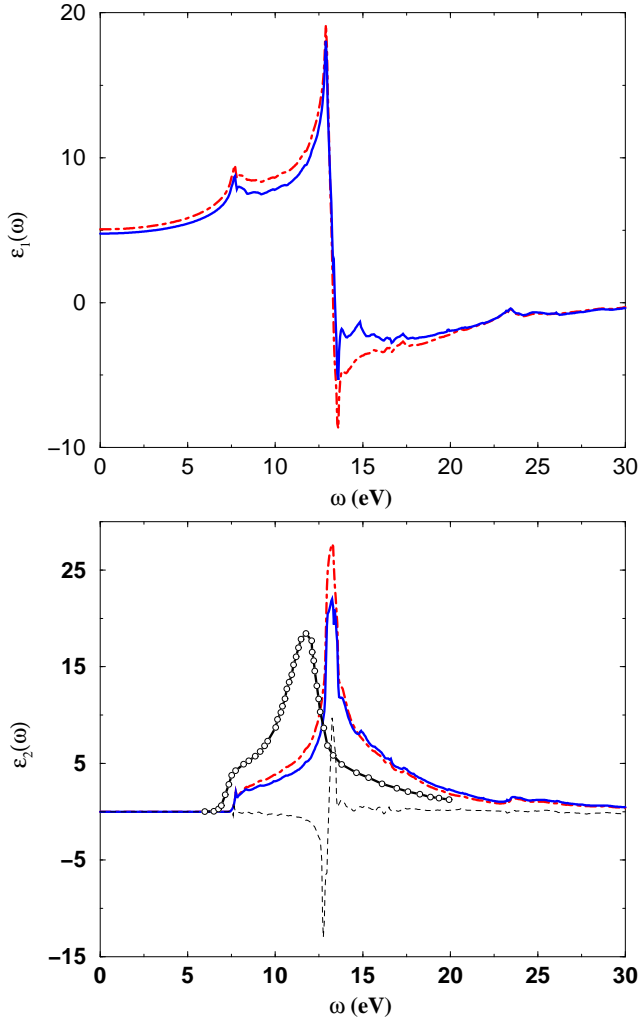


FIG. 8. Calculated real and imaginary part of the Dielectric function of C versus photon energy. The dot-dashed line is our calculation using the quasiparticle energies. The solid line is our calculation using the quasiparticle energies and including the local-field effects. The solid line with open circles is the experimental spectrum⁴⁵. The dashed curve represents the difference between the calculations using the quasiparticle energies and the LDA calculation with a GW rigid energy shift of 1.9 eV of the conduction states. This rigid energy shift corresponds to the GW correction of the band gap at the Γ point.

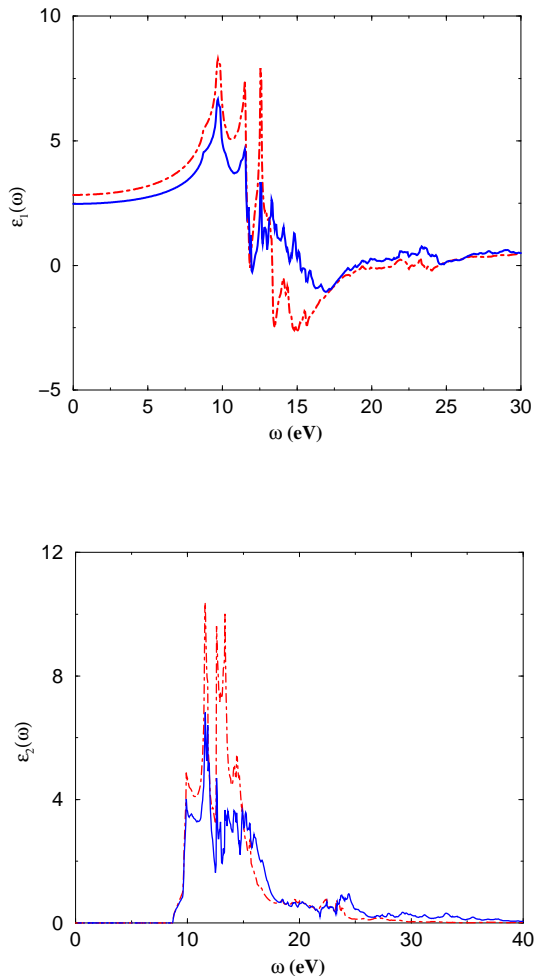


FIG. 9. Calculated real and imaginary part of the dielectric function of LiCl versus photon energy. The dot-dashed line is our calculation using a rigid energy shift of 2.8 eV of the LDA conduction bands, corresponding to our calculated GW band gap correction at the Γ point. The solid line is our calculation with a rigid energy shift and including the local-field effects.

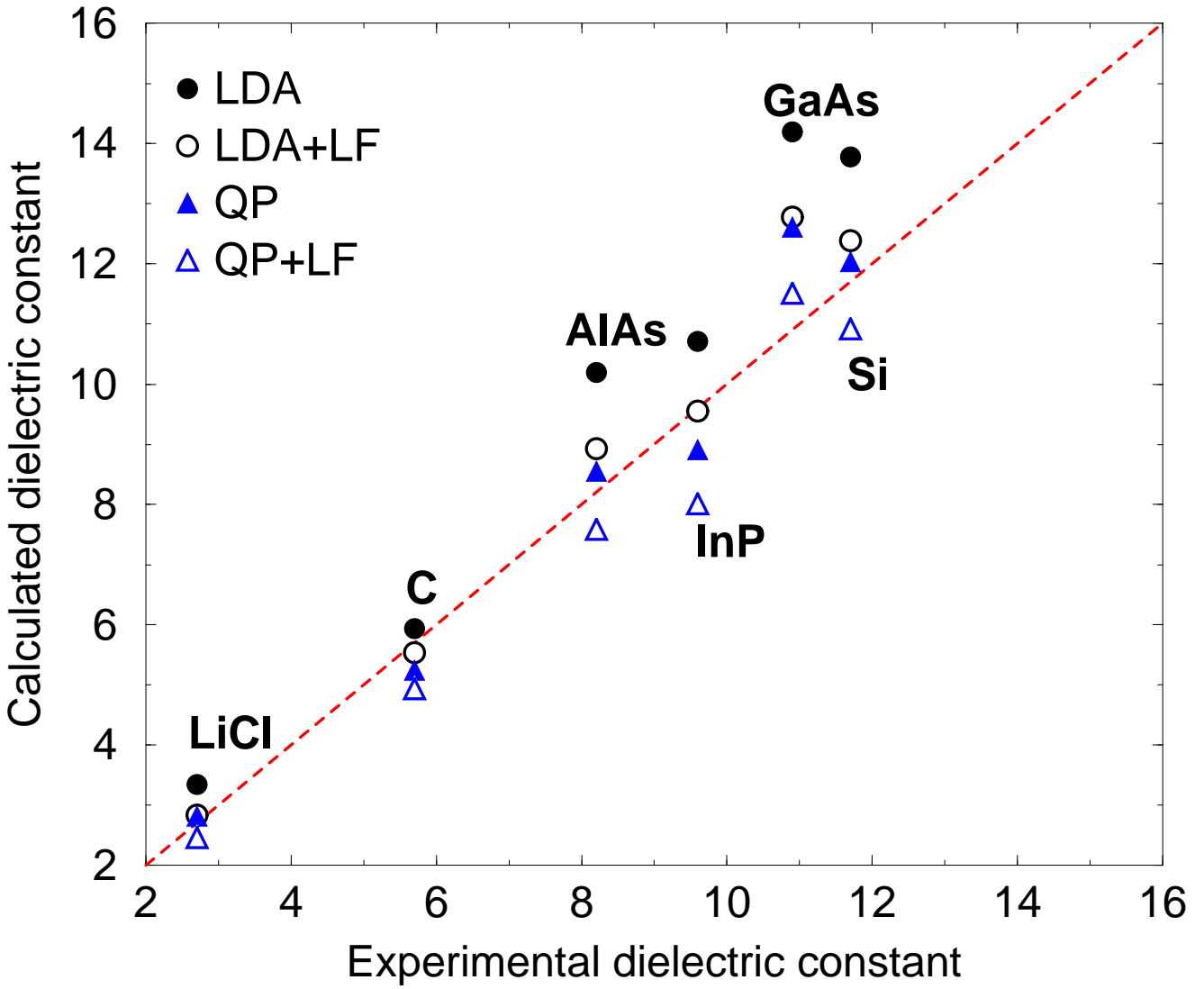


FIG. 10. Calculated static dielectric function compared to experimental results. The filled circles represent the LDA values without local-field effects (LF), the open circles the LDA values with LF and the up-triangles the LDA without LF but with an energy shift corresponding to the GW correction of the direct band gap at the Γ point, the empty up-triangles are the LDA values with the GW energy shift and the LF (see text). A perfect agreement with experiment is achieved when a calculated value is on the dashed line. Notice that when the GW energy shift and the LF are included the calculation underestimates the static dielectric constant for all these semiconductors regardless of the size of the band gap. This suggest the importance of the excitonic effects which are expected to produce a positive correction leading to a better agreement with experiment.

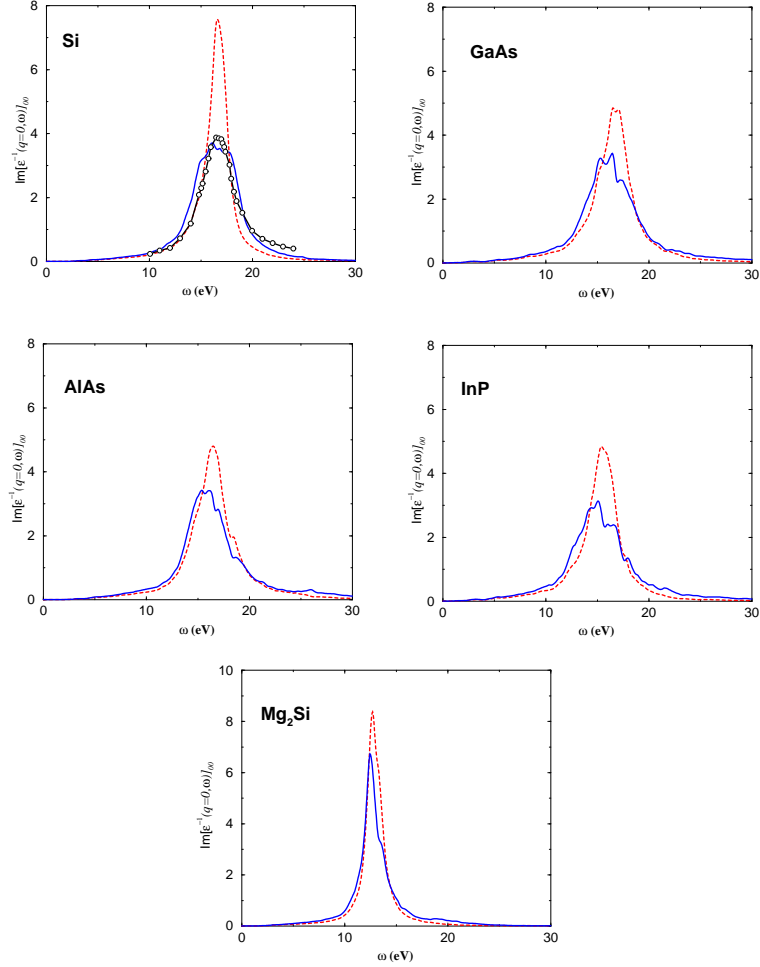


FIG. 11. Calculated energy loss function with (solid line) and without local-field effects (dashed line) of small and medium band-gap semiconductors: Si, GaAs, AlAs, and Mg_2Si compared to available experimental results⁴¹ (solid line with open circle).

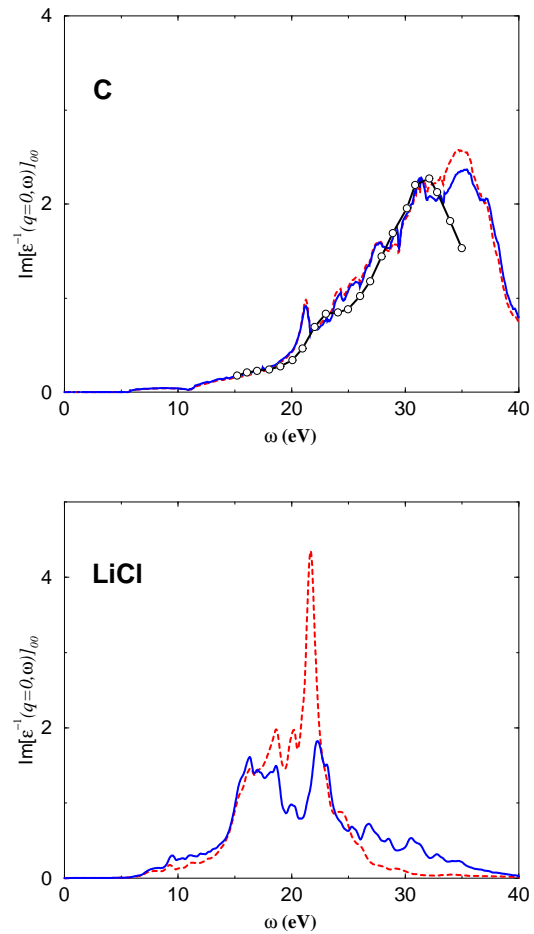


FIG. 12. Calculated energy loss function with (solid line) and without local-field effects (dashed line) of large band gap semiconductors: C and LiCl compared to available experimental results⁴² (solid line with open circle).